INFLUENCE OF LEWIS BASE IDENTITY ON RATES OF MULTIDENTATE LIGAND EXCHANGE

by

Taylor F. Nelson

A thesis submitted in partial fulfillment of the requirements for graduation with Honors in Chemistry.

Whitman College
2014

Certificate of Approval

This is to certify that the accompanying thesis by Taylor F. Nelson has been accepted in partial fulfillment of the requirements for graduation with Honors in Chemistry.

_____
Dr. Nathan E. Boland

Whitman College
May 14, 2014

Table of Contents

Abstract

Ligand exchange reactions influence the geochemical speciation of transition metal and chelating agents, which in turn affects bioavailability, solubility, and mobility of nutrient and contaminant metals. Chelating agents containing phosphonate groups are especially relevant because they are widely used as corrosion inhibitors, medications, and detergent builders. Here, we examine the influence of phosphonate Lewis base groups on ligand exchange rates. We employ capillary electrophoresis with spectrophotometric detection to follow the kinetics of nickel (II) capture by a strong chelating agent (CDTA) from weaker amino(phosphono)carboxylate chelating agents. A suite of structurally related chelating agents are examined. Replacing carboxylate groups with phosphonate groups increases chelating agent basicity and alters the pH-dependence of reaction rates. The influence of chelating agent structure on rates and pathways of ligand exchange are discussed.

List of Figures

List of Tables

1. Introduction

1.1 The role of Ni(II) in the environment

Nickel plays an important role in biological processes and systems. Since 1975, it has been accepted that nickel serves as the active site in the enzyme urease,[1] which catalyzes the hydrolysis of urea, and is thus an essential protein in many plants.[2] Brown et al.[3] demonstrated the importance of nickel concentration in the growth media of grain producing plants, such as barley, to their germination.

Heavy metals such as nickel can also have harmful effects on the environment. Concentrations of only 1-2 ppm of nickel can be toxic to some plant species.[4] Kukier and Chaney[5] also reported great decreases in yield for various crop bearing species in farms near a nickel refinery where the soil concentration of nickel was measured at 1-5 ppm.

1.2 Chelating agents

The term “chelating agent” describes a ligand which forms a complex with a metal ion via multiple coordination bonds. These ligands are also referred to as a multidentate ligand. Metal complexes formed by chelating agents gain extra stability compared to those formed by monodentate ligands with the same donor atom groups. For example, a Cd(II) complex with two ethylenediamine ligands (bidentate) has a higher stability constant ($\log \beta = 10.62$) than a Cd(II) complex with four methylamine ligands (monodentate) ($\log \beta = 6.55$), even though each complex is composed of the same atoms (Figure 1).[6]

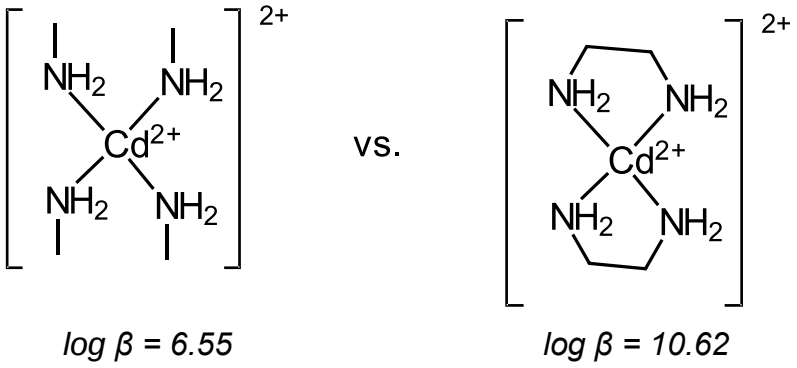

Figure 1. Structures of tetrakis(methylamine) cadmium (II) and bis(ethlyenediamine) cadmium (II) and their respective stability constants.

The only structural difference is the closed rings formed by the ethylenediamine ligands coordinating Cd(II). When comparing the formation of these two different complexes, there is no difference in enthalpy, but a favorable change in entropy for closed ring formation, called the "chelate effect".[6,7]

The coordinating properties of chelating agents are useful for many applications involving the complexation of metals. Some chelating agents are naturally occurring molecules which are released by plants to facilitate metal uptake. One such chelating agent, rhizoferrin, is secreted by fungi to capture metal ions in soil.[8,9] Other chelating agents are synthetic molecules with a variety of applications, including the inhibition of calcium sulfate scale formation on pipes.[10] The widespread use of chelating agents means they are ubiquitous in the environment, so it is important to understand the impacts their presence has on the systems in which they interact.

1.3 Ni(II) complexes / Interactions of Ni(II) with chelating agents

An increased understanding of speciation of both nickel and chelating agents leads to a better understanding of their bioavailability, mobility, and degradation. Hyperaccumulators are plant species which can tolerate high levels of heavy metals, and their use in heavy metal remediation from contaminated soils has been investigated.[11] As demonstrated by Centofanti et al.,[12] the uptake of nickel by hyperaccumulator plant species depends on the solubility of nickel, which in turn depends on its speciation. In hyperaccumulator plants, the speciation of Ni(II) is dominated by organic acids (chelating agents containing carboxylate and amine coordinating atoms) when they are present.[13] By forming complexes with metal ions, chelating agents increase the mobility of metals. To take advantage of this behavior, the use of chelating agents to remediate soils contaminated by heavy metals has been explored; however, the use of some chelating agents, such as EDTA, raises concerns because of their low biodegradability.[14]

1.4 Multidentate ligand exchange

Metals and chelating agents both play important roles in the environment as vital actors in biological and physical processes. Complexes can act as metal ion shuttles in soil for plant uptake as long as the complexes have low enough thermodynamic stability to release the metal ions and high enough kinetic lability to undergo ligand exchange reactions within the relevant timescale.[15] For certain plants, this timescale is their exudation cycle of chelating agents: plants release

chelating agents, which capture metals and are then taken up again by the plants. This process usually occurs within the range of less than six hours per day,[16] falling within the time scale on which multidentate ligand exchange reactions occur.[17] If the exudation/uptake process occurred on a faster time scale than those of exchange reactions, information about the initial speciation of the system would be sufficient for understanding the extent and identity of metal taken up by the plant. On the other hand, if the process was much slower than exchange reactions, the system would be allowed to reach equilibrium prior to uptake; therefore, knowing the equilibrium speciation would be sufficient. Speciation information about the kinetics of multidentate ligand exchange reactions is the only way to accurately predict the speciation of the system throughout processes such as exudation/uptake cycles.

Although it may seem as though the kinetics of multidentate ligand exchange reactions can be predicted by the rates of water exchange for the relevant metal ion, this is not the case. Rates of water exchange for most of the common transition metals (Mn(II), Fe(II) Co(II), Ni(II), Fe(III)) fall within a small range (10^4-10^7 sec) and depend only on the identity of the metal.[18] Conversely, research on various multidentate ligand exchange reactions involving Ni(II) has shown a wide range of exchange rates, and a dependence on the structure of the ligands forming the initial and equilibrium complexes.

1.5 Structure-reactivity relationships

An important aspect of environmental chemistry is the ability to predict the behavior of chemicals present in the environment. This can be challenging for substances which have not been well-characterized or are placed in novel conditions, and is especially important in the design of new chelating agents, which are usually developed to serve a specific purpose or exhibit a certain behavior. Predictive relationships between structural features and reactivity are developed by comparing experimental results between chelating agents which vary in only one aspect of structure. For this reason, the current research project focuses on a series of chelating agents that differ by Lewis base identity. This series was designed by starting with a chelating agent whose multidentate ligand exchange behavior has been studied (NTA)[17] and using the derivatives with a varying number of phosphonate groups replacing carboxylate groups (Figure 2).

Because phosphonates are stronger Lewis bases than carboxylates, these changes had effects on the complexation with Ni(II) which are vital in understanding the reactive behavior of these compounds and are discussed later. Collecting kinetic data allows us to compare ligand exchange reactivity of these different chelating agents, and develop structure-reactivity relationships.

1.6 Ligand exchange mechanisms

Generally, ligand exchange mechanisms fall into three classes, outlined most notably by Langford and Gray.[19] These mechanistic classes are: dissociative, characterized by an intermediate with a decreased coordination

Chelating agent	Free form (protonation at pH = 7)	Ni(II) complex (fully deprotonated)
NTA nitrilotriactetic acid	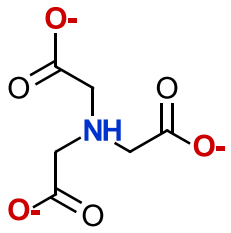	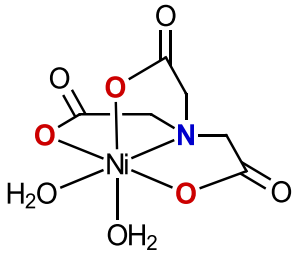
PMIDA N-(phosphonomethyl) iminodiacetic acid	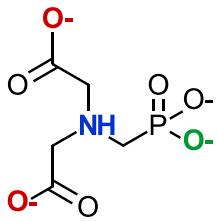	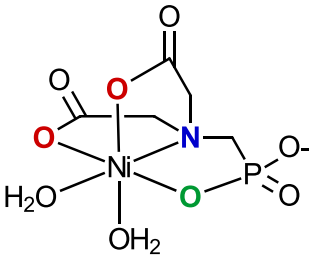
BPMG N,N-bis(phosphono-methyl)glycine	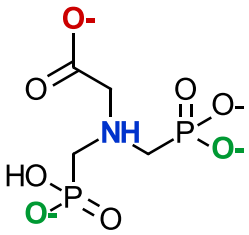	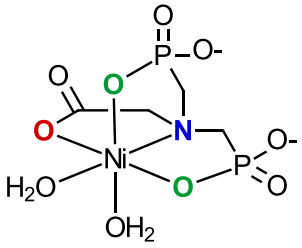
NTMP nitrilotrimethyl-phosphonic acid	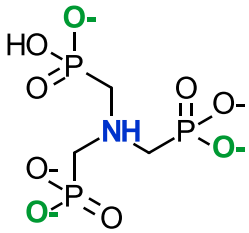	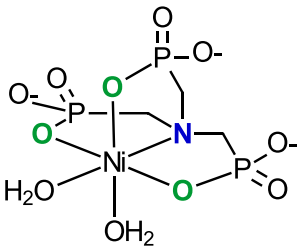

Figure 2. Structures of amino(phosphono)carboxylate chelating agents and their Ni(II) complexes.

number; associative, characterized by an intermediate with an increased coordination number; and interchange, which has no well-defined intermediate. These mechanisms designate elementary steps in multidentate ligand exchange, but because of the large number of steps in a multidentate ligand exchange reaction, more generalized reaction pathways are needed to describe them. Based on recent research, three possible pathways for exchange reactions between two aminocarboxylate multidentate ligands have been proposed (Figure 3).[17] For multidentate ligand exchange pathways involving Ni complexes with amine-containing multidentate ligands, it can be assumed that the dissociation of water is not the rate determining step, since the dissociation of the Ni-N bond is slower. Additionally, Ni-O bonds to carboxylate groups are much more labile than Ni-N bonds. The lability of Ni-O bonds to phosphonate groups has not been directly investigated, but results from this research may be used to compare the relative dissociation of carboxylate groups and phosphonate groups. We hypothesize that phosphonate groups should be even more labile than carboxylate groups, if the lability depends on the "softness" of the base.

For each pathway, there is also the possibility for a parallel proton promoted pathway to occur. The proton promoted pathways involve an incoming proton competing with the complexed Ni(II) ion for a bond on one arm of the initial multidentate ligand (L). This action accelerates either the full or partial dissociation of L from NiL or an intermediate containing Ni and L. With the assumption that these proton promoted pathways are occurring simultaneously with the "normal" pathways, it is expected that each will produce a separate

kinetic term for the formation of NiY. Additionally, the dissociation rate of NiY can be ignored, since it is very slow relative to other rates. The rate of reaction via each pathway depends on steps and the intermediates formed, and are outlined below as derived by Boland.[20] The first pathway, termed “disjunctive,” involves the slow, full dissociation of the initial ligand from the metal:

$$NiL \rightleftharpoons Ni + L \qquad k_1, k_{-1} \qquad (1)$$

followed by the fast formation of the complex with the incoming ligand:

$$Ni + Y \rightarrow NiY \qquad k_2 \qquad (2)$$

Using the steps and assumptions outlined above, the rate of formation of NiY for this pathway can be defined as

$$\frac{d[NiY]}{dt} = \frac{k_1 k_2 [NiL][Y]}{k_{-1}[L] + k_2[Y]} \qquad (3)$$

When the proton promoted dissociation of L from NiL is considered:

$$NiL + H^+ \rightleftharpoons Ni + HL \qquad k_1^H, k_{-1}^H \qquad (4)$$

the rate of NiY formation will have an added term for the dependence on this step:

$$\frac{d[NiY]}{dt} = \frac{k_1 k_2 [NiL][Y]}{k_{-1}[L] + k_2[Y]} + \frac{k_1^H k_2 [NiL][Y][H^+]}{k_{-1}[HL] + k_2[Y]} \qquad (5)$$

The second pathway, termed “interjunctive,” involves the partial dissociation of the initial ligand from the metal:

$$NiL \rightleftharpoons NiL' \qquad k_3, k_{-3} \qquad (6)$$

followed by the partial binding of the incoming ligand to the metal:

$$NiL' + Y \rightleftharpoons NiL'Y' \qquad k_4, k_{-4} \qquad (7)$$

and finally the full dissociation of the initial ligand along with the full complexation by the incoming ligand:

NiL'Y' → NiY + L k_5 (8)

For this pathway, it can be assumed that the consumption of the intermediates NiL' and NiL'Y' is much more rapid than their formation. Therefore, they should not accumulate in significant amounts, and their concentrations can be replaced using the steady state approximations:

$$[NiL']_{ss} = \frac{k_3[NiL]}{(k_4[Y] + k_{-3})}$$

and

$$[NiL'Y']_{ss} = \frac{k_4[NiL']_{ss}[Y]}{(k_5 + k_{-4})} = \frac{k_4 k_3[NiL][Y]}{(k_5 + k_{-4})(k_4[Y] + k_{-3})}$$

Using the steps and assumptions outlined above, the rate of formation of NiY for this pathway can be defined as

$$\frac{d[NiY]}{dt} = k_5[NiL'Y']_{ss} = k_5\frac{k_4 k_3[NiL][Y]}{(k_5 + k_{-4})(k_4[Y] + k_{-3})} \quad (9)$$

When the proton promoted steps for this pathway are considered:

NiL + H^+ ⇌ NiHL' k_3^H, k_{-3}^H (10)

NiHL' + Y ⇌ NiHL'Y' k_4^H, k_{-4}^H (11)

NiHL'Y' → NiY + HL k_5^H (12)

the rate of NiY formation will have an added term for the dependence on this step:

$$\frac{d[NiY]}{dt} = \frac{k_5 k_4 k_3[NiL][Y]}{(k_5 + k_{-4})(k_4[Y] + k_{-3})} + \frac{k_5^H k_4^H k_3^H[NiL][Y][H^+]}{(k_5^H + k_{-4}^H)(k_4^H[Y] + k_{-3}^H)} \quad (13)$$

Finally, the third pathway, termed “adjunctive,” involves first the binding of the incoming ligand to the initial metal complex:

$$NiL + Y \rightleftharpoons NiLY' \qquad k_6, k_{-6} \qquad (14)$$

followed by the dissociation of the initial ligand and the completion of complexation by the incoming ligand:

$$NiLY' \rightarrow NiY + L \qquad k_7 \qquad (15)$$

For this pathway, it can be assumed that the consumption of the intermediate NiLY’ will be much more rapid than its formation, so it should not accumulate in a significant amount. Therefore, its concentration can be replaced by the steady state approximation:

$$[NiLY']_{ss} = \frac{k_6[NiL][Y]}{k_{-6} + k_7}$$

Using the steps and assumptions outlined above, the rate of formation of NiY for this pathway can be defined as

$$\frac{d[NiY]}{dt} = k_7[NiLY']_{ss} = k_7\frac{k_6[NiL][Y]}{k_{-6} + k_7} \qquad (16)$$

When the proton promoted dissociation of L from NiL’Y is considered:

$$NiLY' + H^+ \rightarrow NiY + HL \qquad k_7^H \qquad (17)$$

the rate of NiY formation will have an added term for the dependence on this step:

$$\frac{d[NiY]}{dt} = \frac{k_7k_6[NiL][Y]}{k_{-6} + k_7} + \frac{k_7^Hk_6[NiL][Y][H^+]}{k_{-6} + k_7^H[H^+]} \qquad (18)$$

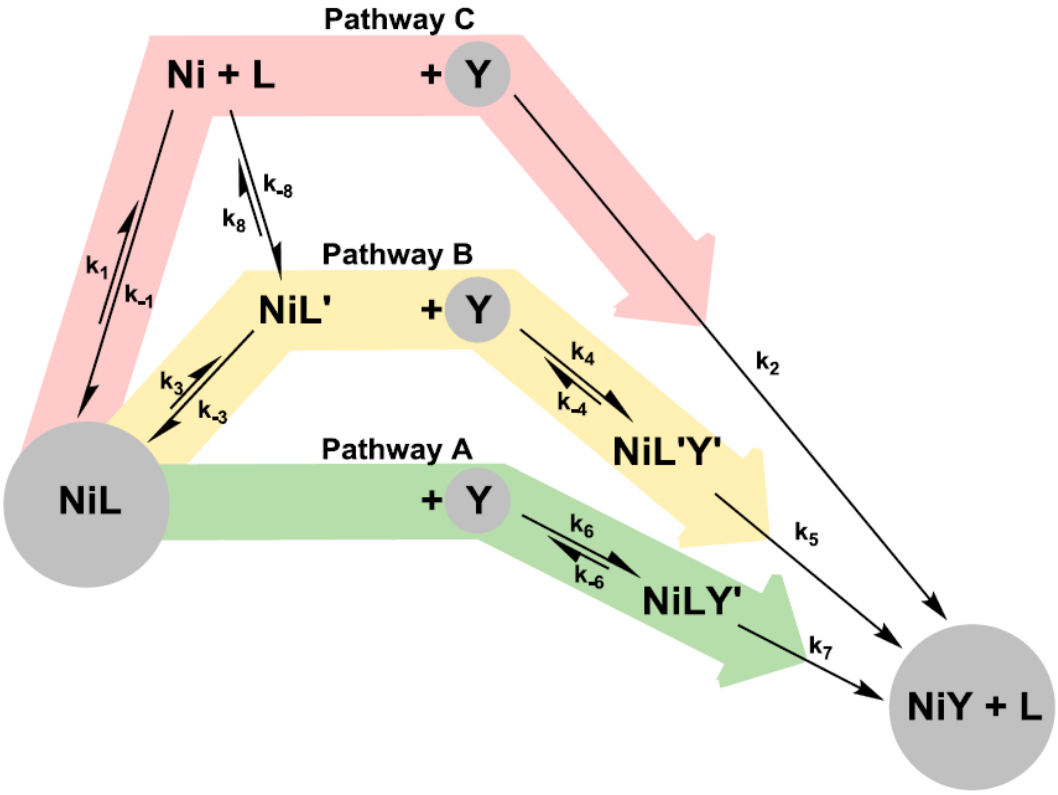

Figure 3. (Figure 4.13 from ref. 17) Three overall pathways of multidentate ligand exchange. Note: The apostrophe (') indicates a ligand that is partially chelated. Reactants and products are highlighted with gray circles.

Boland previously examined Ni(II) capture by EDTA and CDTA from a range of initial aminocarboxylate-Ni(II) complexes.[17] EDTA and CDTA, which vary only in the addition of a cyclohexane on the N-N bridge in CDTA, were both used as incoming ligands in separate experiments to observe the effects of rigidity on the ligand exchange reaction (Figure 4). The cyclohexane connecting the amine groups on CDTA forces the carboxylate arms into a more rigid conformation. Boland noted that this rigidity resulted in steric hindrance between these arms, making the formation of a ternary complex during ligand exchange unlikely when a tetradentate, tripodal ligand (such as NTA) is already bound to the metal ion.

Chelating agent	Free form (protonation at pH = 7)	Ni(II) complex (fully deprotonated)
EDTA ethylenediamine-tetraacetic acid	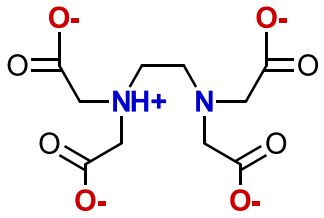	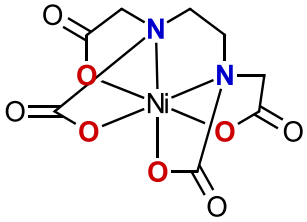
CDTA trans-cyclohexane-ethylenediamine-tetraacetic acid	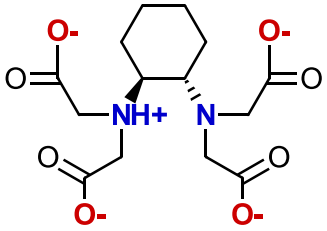	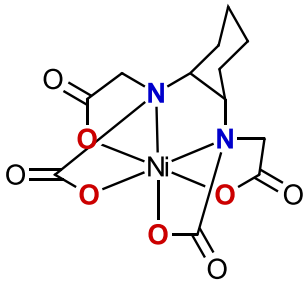

Figure 4. Structures of EDTA and CDTA, used as incoming chelating agents in selected ligand exchange reactions.[17]

Therefore, at least partial dissociation of the initial tetradentate, tripodal ligand is required prior to the complexation between the metal and CDTA. Furthermore, faster exchange rates were observed when EDTA was used as the incoming ligand compared to CDTA. This result supported the assertion that CDTA is incapable of forming NiCDTA without initial (*at least* partial) dissociation of the original ligand. Because EDTA is less sterically hindered, it can capture Ni(II) without dissociation of the initial complex, resulting in a much faster reaction. In another experiment, several reaction conditions were varied to determine their effects on the rate of the following exchange reaction:

NiNTA + CDTA --> NiCDTA + NTA (19)

Boland observed that varying the amount of CDTA had no effect on the reaction rate, suggesting that CDTA is not involved in the rate determining step. Additionally, increasing the pH of the reaction sample produced a sharp decrease in rate. Boland proposed that there is a significant influence of the proton-promoted pathway, as the dependence on pH indicated a dependence of the rate on $[H^+]$. The conclusions from past research[17] led to the proposal of the disjunctive pathway for reaction (19) (Figure 5), which will inform the conclusions of the current research. The chelating agents being investigated here are structural derivatives of NTA, and are likely to follow a similar reaction pathway.

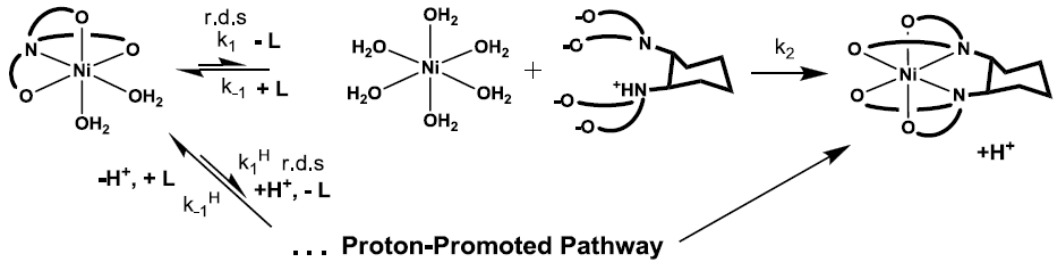

Figure 5. (Figure 4.7 from ref. 17) Reaction between Ni(II)-tripodal chelating agent complexes and CDTA.

1.7 Capillary electrophoresis theory

Capillary electrophoresis is an ideal method for quantitatively monitoring multidentate ligand exchange reactions. By combining electrophoretic separation with UV-vis absorbance detection, capillary electrophoresis allows for the simultaneous separation and analysis of multiple species based on size and charge. Therefore, every separation contains information about the concentration

of multiple species in the sample, providing a snapshot of the reaction progress. This is a great advantage over analytical chemical techniques which only allow for analysis of the bulk solution (such as conventional UV-vis detection) as well as those which separate species based on interactions between the analyte(s) and a stationary phase (such as HPLC) that could impact the complexation of metal ions with chelating agents. The output of an electrophoretic separation, an electropherogram (Figure 6), contains an absorbance peak for multiple charged analytes in solution, as well as "system peaks" caused by ionic constituents of the BGE.[21] The ratio of (peak area) / (retention time) for each is directly proportional to the concentration of the corresponding ion.

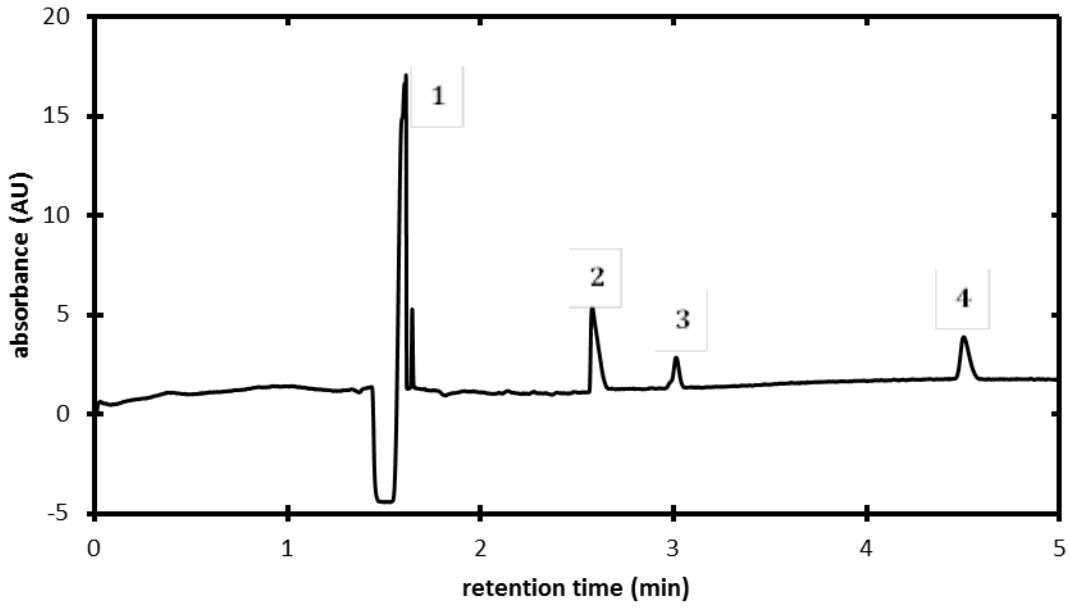

Figure 6. Example electropherogram. Solution conditions: 50 µM $Ni(II)_T$, 52.5 µM NTA_T, 200 µM $CDTA_T$, 5 mM MOPS (pH = 7.0), ionic strength = 10 mM. Separation conditions: -22 kV applied voltage, BGE = 20 mM pyrophosphate (pH = 7.0), 0.4 mM TTAB. Assigned peaks: **1** – system peak, **2** – $CDTA_{free}$, **3** – NiCDTA, **4** – NiNTA.

A basic CE set up involves two vials containing an ionic buffer solution, called the background electrolyte (BGE), which are connected by a fused silica capillary. When a potential is applied across the two vials, the charged ions of the BGE respond to the external electric field, and flow through the capillary. This phenomenon is termed electroosmotic flow. If a sample solution is injected into the capillary prior to the application of this potential, then its components will also flow through the capillary, but with different velocities.

The velocity of the ions in the capillary can be expressed as:

$$\nu = \mu * E \tag{20}$$

in which E represents the strength of the applied electric field and μ represents the electrophoretic mobility of the ion, which in turn can determined by the following relationship:

$$\mu = \frac{q}{6\pi\eta r} \tag{21}$$

in which q represents the charge of the ion, r represents its radius, and η represents the viscosity of the buffer solution.[22]

The introduction of a sample solution into the capillary affects the environment of the capillary by creating system zones, which arise once there are sections of the solution within the capillary that have different compositions. As these system zones move through the capillary, their electroneutrality and conductivity must remain constant, even as ions move in and out of the zones. This results in disturbances in the electropherogram that appear as peaks and troughs.

The selection of BGE solution is an important aspect of CE separations. Most importantly, the BGE ions should not readily form complexes with the metal(s) being analyzed. For analytes which do not have significant UV absorbance, and thus cannot be directly analyzed, indirect detection must be used. This limits the scope of possible BGEs, as indirect detection requires a highly absorbing BGE. As analyte ions displace BGE ions from their system zone, a difference in absorbance between the BGE and analyte ions can be measured. Alternatively, for analytes with significant UV absorbance (such as carboxylate-containing chelating agents and their Ni(II) complexes), a low UV absorbing BGE can be used. This method is appropriately termed direct detection, as the absorbance of the analytes is directly measured. Direct detection is advantageous because it produces less noisy baselines than indirect detection.

1.8 Research model

The goal of this research is to determine the impact of Lewis base group identity on the ligand exchange reactivity of chelating agents by investigating multidentate ligand exchange reactions with NTA-like amino(phosphono)-carboxylate chelating agents as initially complexed ligands and CDTA as an incoming ligand. Foremost, the Ni(II) speciation in the presence of different chelating agents must be investigated to guide interpretation of kinetic data. Methods for analyzing Ni(II) complexes with multidentate aminocarboxylate ligands using CE will be adopted[23–27] and used to determine the initial rate of

formation (defined as the first 20% of the reaction) of NiCDTA over time for various ligand exchange reactions. These reaction rates will be compared to the reaction rate for the parent compound NTA, which has been experimentally determined.[20] This comparison will ultimately inform the development of structure-reactivity relationships for these multidentate chelating agents, as well as the possible reaction pathways the exchange reactions take.

2. Materials & Methods

2.1 Reagents

Reagent grade chemicals and 18 MΩ cm resistivity ultra-pure water generated by a Milli-Q water purification system (Millipore; Billerica, MA) were used for preparation of all solutions and in operation of the capillary electrophoresis system.

Nickel (II) chloride, nitrilotriacetic acid trisodium salt (NTA), and trans-1,2-diaminocyclohexane-N,N,N',N'-tetraacetic acid monohydrate (CDTA) were purchased from Alfa Aesar. Sodium chloride, N-(phosphonomethyl)iminodiacetic acid (PMIDA), N,N-bis(phosphonomethyl)glycine (BPMG), and nitrilotrimethyl-phosphonic acid (NTMP), were purchased from Sigma-Aldrich. 3-(N-morpholino)-propanesulfonic acid (MOPS) was purchased from JT Baker. Tetradecyl trimethyl ammonium bromide (TTAB) was purchased from Amresco. Sodium acid pyrophosphate was purchased from Spectrum.

2.2 Sample preparation

Class A glassware was acid washed in 5M HNO_3 and rinsed with ultra-pure water before being used to prepare solutions, which were then stored in polypropylene bottles at 4°C.

Stock solutions of nickel chloride, various chelating agents, and buffers were prepared in class A glassware. Nickel chloride solutions were made acidic (pH~5) with small amounts of HCl to prevent adsorption to container surfaces and formation of hydroxo species.

Sample solutions of nickel-chelating agent complexes were prepared from stock solutions. Each sample contained 5 mM of a pH buffer and 8 mM NaCl to raise the ionic strength to 10 mM. Samples were prepared at least an hour before they were analyzed to ensure they had reached equilibrium.

2.3 Capillary electrophoresis

Analyses were performed using a G1600 (Agilent; Santa Clara, CA) or a P/ACE MDQ (Beckman-Coulter; Brea, CA) capillary electrophoresis system employing a diode array UV detector and with temperature control keeping the sample vial holder and capillary at 25°C.

The kinetics of the ligand exchange reactions were determined by monitoring the formation of NiCDTA. This formation rate was determined from measuring concentration based of the ratio of (peak area / retention time) from the absorption electropherogram at 214 nm.

Separations were performed in an underivatized fused silica capillary with a 75 µm inner diameter and a total length of 47.5 cm. A portion of the coating was removed from the capillary 40 cm from the injection end by warm sulfuric acid with the aid of a window etching tool (Agilent) to create a uniform window for UV detection. A simpler method for creating the detection window involves the use of a flame to remove the polyimide coating. However, doing so can distort the capillary which impacts its optical properties.[28] Each day, the capillary was preconditioned with a 5 minute rinse with 0.1 M NaOH, a 2 minute rinse with ultra-pure water, then a 15 minute rinse with the background electrolyte (BGE) solution being used in the analysis. Between each separation, the capillary was rinsed with ultra-pure water for 1 minute, then BGE solution for 1 minute. Rinses were performed by applying pressure of 930 mbar. Each separation began with a pressure injection of the sample at 35 mbar for a fixed amount of time, and then a voltage of between -22 kV and -30 kV was applied for a set interval of time.

BGE solutions were composed of an electrolyte buffer (concentration ranging from 10-50 mM) and a low concentration of TTAB (0.25-0.5 mM). The purpose of the electrolyte was to buffer the pH and ionic strength of the capillary environment, as well as allow for the selective separation of anions. TTAB is a surfactant that acts as an electroosmotic flow modifier. The purpose of the modifier was to coat the capillary walls with a net positive charge, reversing the electroosmotic flow to yield facile detection of anions with a negative applied voltage.[24,25] Additionally, the presence of TTAB limited adsorption of the analytes

to the capillary walls.[26] BGE solutions were filtered through polycarbonate track-etch membrane filters (Whatman; Florham Park, NJ) by suction filtration prior to use in the CE system. This procedure was employed to prevent particles and air bubbles from entering the capillary.

3. Results & Discussion

3.1 Analysis by Capillary Electrophoresis - Peak Assignment and Calibration

From the calibration runs, it was possible to assign peaks based on changes in known concentration and inferences about relative migration time (based on size and charge). Analyzing the data, it was determined that NiCDTA produced more reliable absorbance peaks than the other species, so rates were all determined from the rates of NiCDTA formation. Samples were prepared by mixing equal volumes of two solutions: one containing NiL, the other free CDTA. To measure the concentrations of the different species in each kinetics sample over time, each sample was separated multiple times using the methods outlined in the Experimental section. For each series of separations, the instrument was calibrated using external NiCDTA standards.

3.2 Reproducibility Testing

In initial attempts to gather kinetic data, sufficient linear fits ($R^2 > 0.95$) for the initial rate could not be obtained. The issue appeared to be irreproducibility in migration time and peak area across consecutive separations. Reproducibility

tests were performed to isolate the factor which was most affecting the reproducibility migration time and peak area (Table 1). These tests consisted of running six consecutive separations of a single NiCDTA sample (with no reaction taking place), and analyzing the reproduction of peak/area ratio in the generated electropherogram, which theoretically should be consistent between separations. The goal was to achieve a <5% standard deviation in peak/area ratio across the six consecutive separations under a given set of conditions. The following factors were determined to be possible contributors to the irreproducibility and were tested as independent variables:

1) injection time

2) BGE (pyrophosphate) concentration

3) surfactant (TTAB) concentration

Overall, lowering the pyrophosphate (BGE) concentration from 20 mM to 10 mM and TTAB concentration from 0.4 mM to 0.2 mM decreased the standard deviation of area/time between separations. Although pyrophosphate is a good BGE to use because of its low UV absorbance compared to the metal complexes, it was found to have negative effects on the reproducibility of sample peaks. This could be a result of pyrophosphate interactions with the capillary wall affecting the electroosmotic flow. An experiment was performed to determine the rate of exchange between NTA and CDTA (reaction 19) using MOPS as the BGE instead of pyrophosphate, which was used in past experiments (Figure 7).[17]

Table 1. Results of signal reproducibility testing on the Agilent CE system.

[pyrophos] (mM)	[TTAB] (mM)	Inj. Time (sec)	Avg. Area/Time (NiCDTA)	St. Dev.	% Rel. s.d.	n	notes
20	0.4	15	1.0	0.2	16.2%	6	
10	0.25	15	1.05	0.04	**3.6%**	6	
10	0.25	10	2.2	0.2	8.4%	6	
10	0.25	20	5.6	0.2	**3.9%**	6	
20	0.4	15	1.05	0.07	6.9%	12	
20	0.4	10	0.70	0.05	7.8%	6	
20	0.4	20	1.44	0.07	5.0%	6	
10	0.5	15	0.81	0.05	6.1%	6	
10	0.25	15	0.80	0.08	9.6%	6	
10	0.25	15	0.84	0.04	5.2%	6	[1]
10	0.25	15	0.92	0.07	7.4%	6	
10	0.25	15	0.84	0.06	6.6%	6	[2]
10	0.25	15	0.76	0.07	9.6%	6	

[1] For remaining tests, glass separation vials were used instead of plastic
[2] For remaining tests, a vial with H_2O was used as the injection outlet

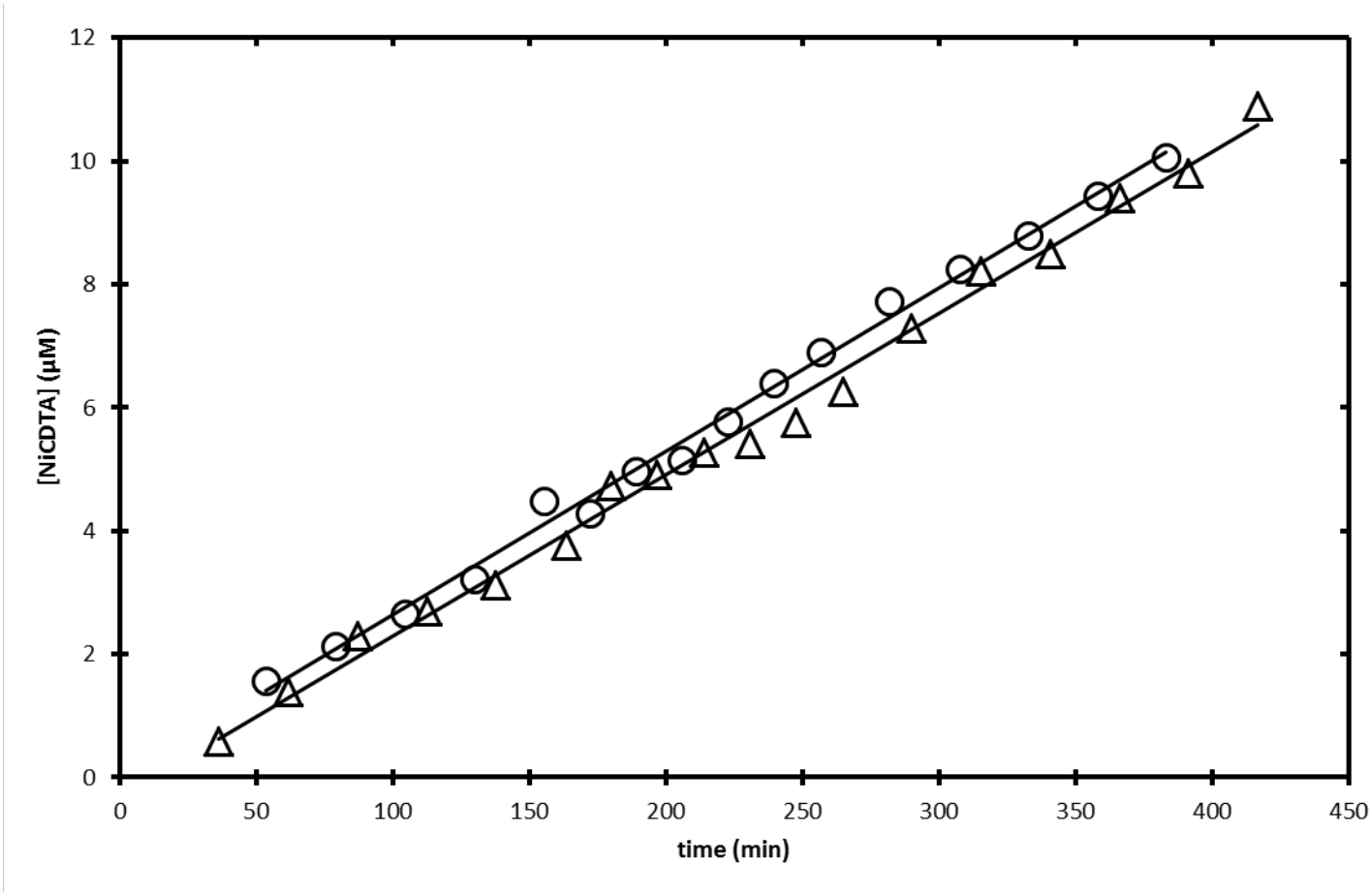

Figure 7. NiCDTA formation over time during ligand exchange with NTA (reaction 19) using MOPS BGE. The linear least squares method was employed to fit the initial rates (**Δ** R^2 = 0.99; **O** R^2 = 0.99). Duplicate experiments are shown. Reaction conditions: 50 µM Ni_T, 52.5 µM NTA_T, 200µM $CDTA_T$, 5 mM MOPS (pH = 7.0), ionic strength = 10 mM

MOPS has a higher UV absorptivity than pyrophosphate, making it less effective for direct detection. However, the results show much better reproducibility between separations than those using pyrophosphate. The rate for this reaction (19) (Ni_T = 50 µM, NTA_T = 52.5 µM, $CDTA_T$ = 200 µM, pH = 7.0, ionic strength = 10 mM) has been determined by Boland as 3.24(±0.30) x 10^{-10} M/s.[20] The rate determined from this experiment, using the same sample conditions, was 4.38(±0.12) x 10^{-10} M/s. This rate is not statistically within the

error of the rates determined previously for the same reaction analyzed using a pyrophosphate BGE. So, although using a MOPS BGE may cause better consecutive separation reproducibility, it may also cause changes in the observed rate. MOPS was used to buffer pH in all sample solutions, so this possibility should be explored further.

3.3 Kinetics Results - NiNTA + CDTA

To validate the experimental setup for determining the rate of multidentate ligand exchange reactions employed in this research, the rate of exchange for reaction between NiNTA and CDTA was determined (reaction 19) using a pyrophosphate BGE. This reaction was performed and analyzed using the methods outlined in the Experimental section and the procedures outlined in Appendix 1, and the rate was determined to be $3.25(\pm 0.21) \times 10^{-10}$ M/s (Figure 8).

The reported uncertainty in each rate is in the slope of concentration vs. time, and was determined using the linear least squares method. The rate determined in this experiment falls within the uncertainty of the reported rate, suggesting that they are statistically indistinguishable, and validating the methods used in this research.

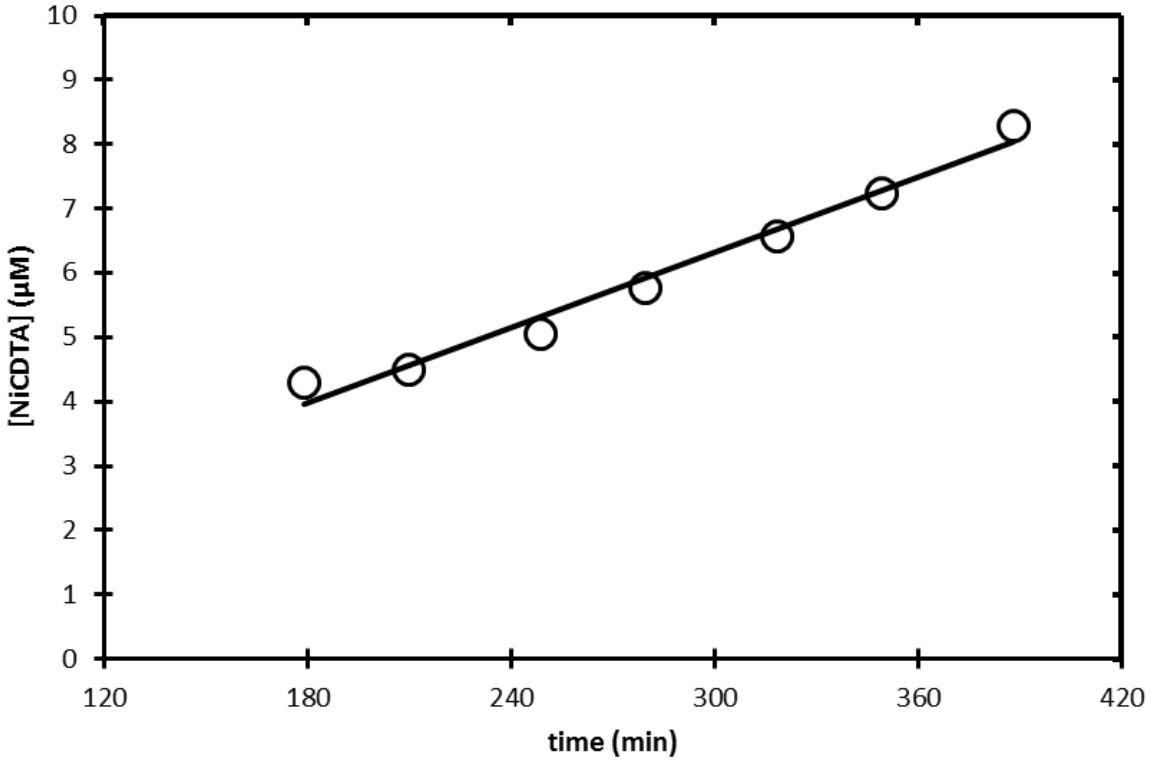

Figure 8. NiCDTA formation over time during ligand exchange with NTA (reaction 19). The linear least squares method was employed to fit the initial rate (R^2 = 0.98). Reaction conditions: 50 µM Ni_T, 52.5 µM NTA_T, 200µM $CDTA_T$, 5 mM MOPS (pH = 7.0), ionic strength = 10 mM.

3.4 Equilibrium speciation of Ni(II) complexes with varying multidentate ligands (L)

As mentioned before, the conversion of carboxylate groups to phosphonate groups in NTA-derivative chelating agents increases Lewis basicity, which in turn impacts complexation with Ni(II). The pK_as for the various chelating agents used as initial ligands are given in Table 2.

Table 2. Relevant acid dissociation constants for chelating agents. Gathered from *NIST* database for conditions: T = 25°C, adjusted to ionic strength = 0.0 M using Davies equation.

Chelating Agent	Equation	log (K_a)
CDTA	$cdta^{4-} + H^+ \rightleftharpoons H(cdta)^{3-}$	13.2
	$H(cdta)^{3-} + H^+ \rightleftharpoons H_2(cdta)^{2-}$	6.73
	$H_2(cdta)^{2-} + H^+ \rightleftharpoons H_3(cdta)^-$	3.94
	$H_3(cdta)^- + H^+ \rightleftharpoons H_4(cdta)^0$	2.70
	$H_4(cdta)^0 + H^+ \rightleftharpoons H_5(cdta)^+$	1.6
NTA	$nta^{3-} + H^+ \rightleftharpoons H(nta)^{2-}$	10.12
	$H(nta)^{2-} + H^+ \rightleftharpoons H_2(nta)^-$	2.96
	$H_2(nta)^- + H^+ \rightleftharpoons H_3(nta)^0$	2
	$H_3(nta)^0 + H^+ \rightleftharpoons H_4(nta)^+$	1
PMIDA	$pmida^{4-} + H^+ \rightleftharpoons H(pmida)^{3-}$	11.46
	$H(pmida)^{3-} + H^+ \rightleftharpoons H_2(pmida)^{2-}$	6.17
	$H_2(pmida)^{2-} + H^+ \rightleftharpoons H_3(pmida)^-$	2.66
	$H_3(pmida)^- + H^+ \rightleftharpoons H_4(pmida)^0$	2.06
BPMG	$bpmg^{5-} + H^+ \rightleftharpoons H(bpmg)^{4-}$	12
	$H(bpmg)^{4-} + H^+ \rightleftharpoons H_2(bpmg)^{3-}$	7.23
	$H_2(bpmg)^{3-} + H^+ \rightleftharpoons H_3(bpmg)^{2-}$	5.63
	$H_3(bpmg)^{2-} + H^+ \rightleftharpoons H_4(bpmg)^-$	2.59
	$H_4(bpmg)^- + H^+ \rightleftharpoons H_5(bpmg)^0$	2.07
NTMP	$ntmp^{6-} + H^+ \rightleftharpoons H(ntmp)^{5-}$	14.3
	$H(ntmp)^{5-} + H^+ \rightleftharpoons H_2(ntmp)^{4-}$	8.41
	$H_2(ntmp)^{4-} + H^+ \rightleftharpoons H_3(ntmp)^{3-}$	6.74
	$H_3(ntmp)^{3-} + H^+ \rightleftharpoons H_4(ntmp)^{2-}$	5.31
	$H_4(ntmp)^{2-} + H^+ \rightleftharpoons H_{5(}ntmp)^-$	1.94
	$H_5(ntmp)^- + H^+ \rightleftharpoons H_6(ntmp)^0$	0.6

The increase in pK_as from NTA to PMIDA (especially that of pK_{a2}, which relates to the new phosphonate group) indicates that PMIDA acts as a stronger base than NTA. This trend continues through the series of chelating agents as phosphonate groups replace carboxylate groups. To determine the effect of this structural change on the complexation with Ni(II), equilibrium speciation calculations were performed (Figure 10) using the computer program HYDRAQL.[29] The relevant formation, dissociation, and solubility constants used in these calculations are given in Tables 2 and 3. These were gathered from the *NIST Critically Selected Stability Constants of Metal Complexes* database.[30] The Davies Equation was used to correct any constants reported at an ionic strength other than zero.

Overall, the calculations show an increase in the pH at which NiL is the predominant species as the number of phosphonate groups is increased. This means that at a constant pH of 7, there is a shift from NiL to NiHL as the predominant species between NTA and NTMP. Literature indicates that the structure of this NiHL complex involves protonation of an O- on the complexing phosphonate arm, which decreases the interaction between this group and the metal cation, compared to a deprotonated carboxylate group (Figure 9).[31]

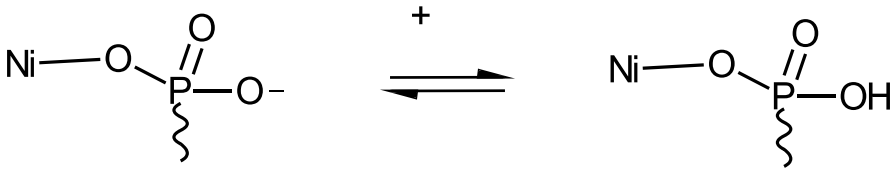

Figure 9. Protonation of phosphonate donor group in NTA- like chelating agents (L = PMIDA, BPMG, NTMP) to form the NiHL complex **.**

Table 3. Relevant equilibrium constants of Ni(II) complexes and precipitates. Gathered from *NIST* database for the conditions: T = 25°C, adjusted to ionic strength = 0.0 M using Davies equation.

Complex	Equation	log (K)
NiCDTA	$Ni^{2+} + cdta^{4-} \rightleftharpoons Ni(cdta)^{2-}$	22.0
	$Ni(cdta)^{2-} + H^{+} \rightleftharpoons NiH(cdta)^{-}$	3.34
NiNTA	$Ni^{2+} + nta^{3-} \rightleftharpoons Ni(nta)^{-}$	12.83
	$Ni^{2+} + 2\ nta^{3-} \rightleftharpoons Ni(nta)_2^{4-}$	16.98
	$Ni(nta)^{-} \rightleftharpoons Ni(OH)(nta)^{2-} + H^{+}$	-11.30
NiPMIDA	$Ni^{2+} + pmida^{4-} \rightleftharpoons Ni(pmida)^{2-}$	13.12
	$Ni^{2+} + 2\ pmida^{4-} \rightleftharpoons Ni(pmida)_2^{6-}$	14.48
	$Ni(pmida)^{2-} + H^{+} \rightleftharpoons NiH(pmida)^{-}$	5.90
	$Ni(pmida)^{2-} \rightleftharpoons Ni(OH)(pmida)^{3-} +$	-12.23
NiBPMG	$Ni^{2+} + bpmg^{5-} \rightleftharpoons Ni(bpmg)^{3-}$	14.2
	$Ni(bpmg)^{3-} + H^{+} \rightleftharpoons NiH(bpmg)^{2-}$	7.01
	$NiH(bpmg)^{2-} + H^{+} \rightleftharpoons NiH_2(bpmg)^{-}$	5.29
NiNTMP	$Ni^{2+} + ntmp^{6-} \rightleftharpoons Ni(ntmp)^{4-}$	15.4
	$Ni(ntmp)^{4-} + H^{+} \rightleftharpoons NiH(ntmp)^{3-}$	8.7
	$NiH(ntmp)^{3-} + H^{+} \rightleftharpoons NiH_2(ntmp)^{2-}$	6.1
	$NiH_2(ntmp)^{2-} + H^{+} \rightleftharpoons NiH_3(ntmp)^{-}$	4.1
NiOH	$Ni^{2+} + OH^{-} \rightleftharpoons NiOH^{+}$	4.1
	$Ni^{2+} + 2\ OH^{-} \rightleftharpoons Ni(OH)_2^{0}$	9
	$Ni^{2+} + 3\ OH^{-} \rightleftharpoons Ni(OH)_3^{+}$	12
	$Ni^{2+} + 2\ OH^{-} \rightleftharpoons Ni(OH)_{2(s,\ am)}$	15.1
	$Ni^{2+} + 2\ OH^{-} \rightleftharpoons Ni(OH)_{2(s,\ cr)}$	17.2

A

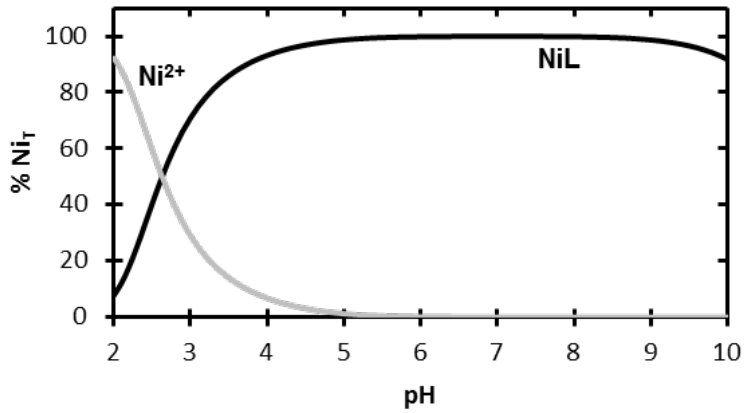

B

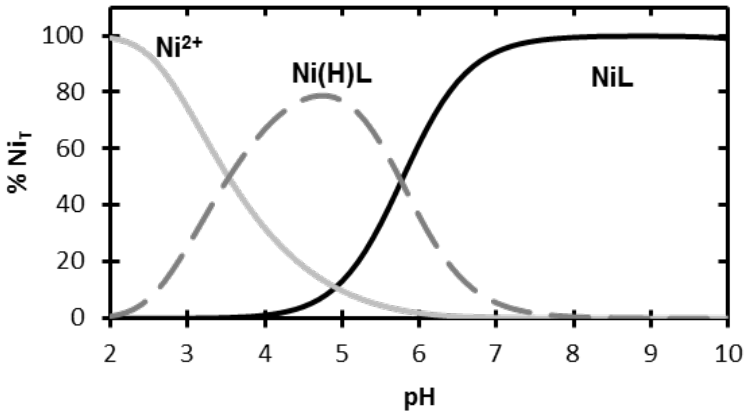

C

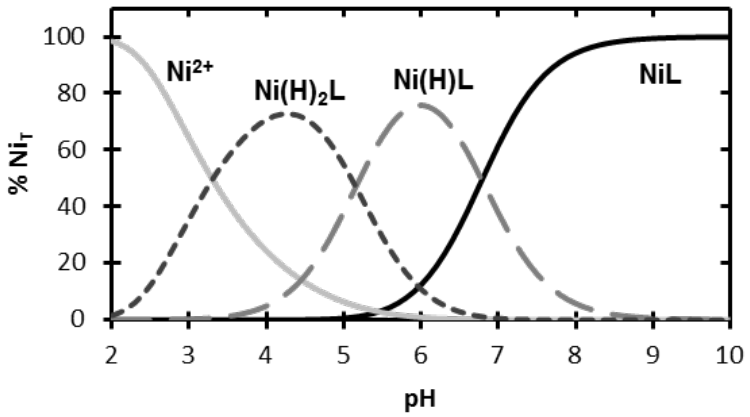

D

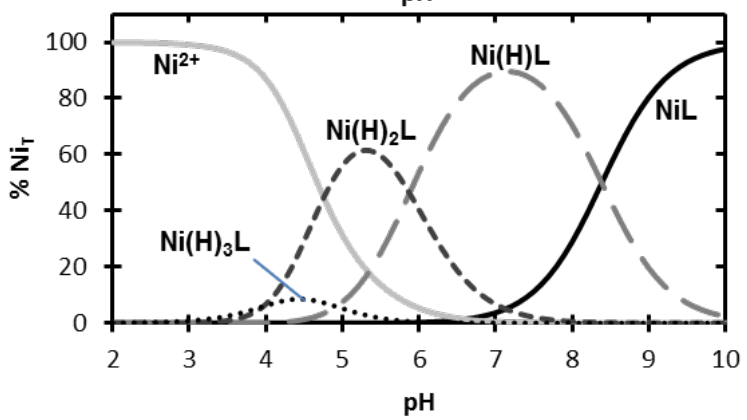

Figure 10A-D. Calculated Ni(II) speciation in the presence of a series of amino(carboxyl)(phosphon)ate ligands (L). **A**: L = NTA; **B**: L = PMIDA; **C**: L = BPMG; **D**: L = NTMP. Solution conditions: Ni_T = 50 µM, L_T = 52.5 µM, ionic strength = 10 mM.

Additionally, the calculations show an increase in free Ni(II) concentration between NTA → NTMP at a constant pH. As the basicity of the chelating agent increases, due to the greater basicity of a phosphonate group than that of a carboxylate group, there is greater competition from protons with Ni(II) ions to complex with the more basic donor groups of the chelating agent. This competition causes an increase in [NiHL] at equilibrium of pH = 7, which increases free Ni(II) concentration. Therefore, though the log K_f increases when phosphonate groups replace carboxylate groups, there is not necessarily an increase in stability of the predominant complex at pH 7. The formation constant K_f only indicates the strength of the NiL complex, which is not necessarily always the predominant species. As seen in Table 2, the value of K_f depends on the concentration of L_{free} (the fully deprotonated form), which will be lower as the pK_a of L increases.

Calculations were also performed using the same conditions as above with the addition of 200 µM $CDTA_T$. The results of these calculations showed that in the presence of CDTA, NiCDTA accounted for more than 99% of the equilibrium speciation of Ni(II). Therefore, the ligand exchange reactions being studied will effectively produce NiCDTA as they move towards equilibrium.

3.5 Kinetics Results - First Separation Data

When multidentate ligand exchange reactions were performed at pH 7.0 using PMIDA, BPMG, and NTMP as the initial ligand, it was found that the amount of NiCDTA formed quickly exceeded the first 20% of the reaction

required for determining the initial rate. Because these values of NiCDTA fell outside of the initial linear range, it was not possible to quantify the rate of reaction. To gather more information about the initial rate, the formation of NiCDTA between the time of reaction initiation and the first possible electrophoretic separation (~160 sec) for each of the four exchange reactions (Figure 11) was measured. Although a single data point is not sufficient for determining a kinetic rate, it can be used to estimate a timescale on which the reactions are occurring, and can be used to evaluate our capillary electrophoresis method as a sufficient method for analyzing these reactions at certain conditions.

For NTA as the initial chelating agent, no detectable amount of NiCDTA had formed by the first separation, as expected based on the slow rate of this reaction. For PMIDA as the initial chelating agent, 6.3(±1.4) μM NiCDTA had been formed, corresponding to about 12.6% reaction completion. Although this first point falls within the first 20% of the reaction, it would be difficult to have three points within the first 20% of the reaction because of the amount of time between separations. For BPMG or NTMP as the initial chelating agent, the reaction had already exceeded 95% completion by the time of the first separation. This implies that the reaction will have to be drastically slowed down, or monitored using an alternative method to CE. Both of these possibilities will be discussed in “Notes for future research.”

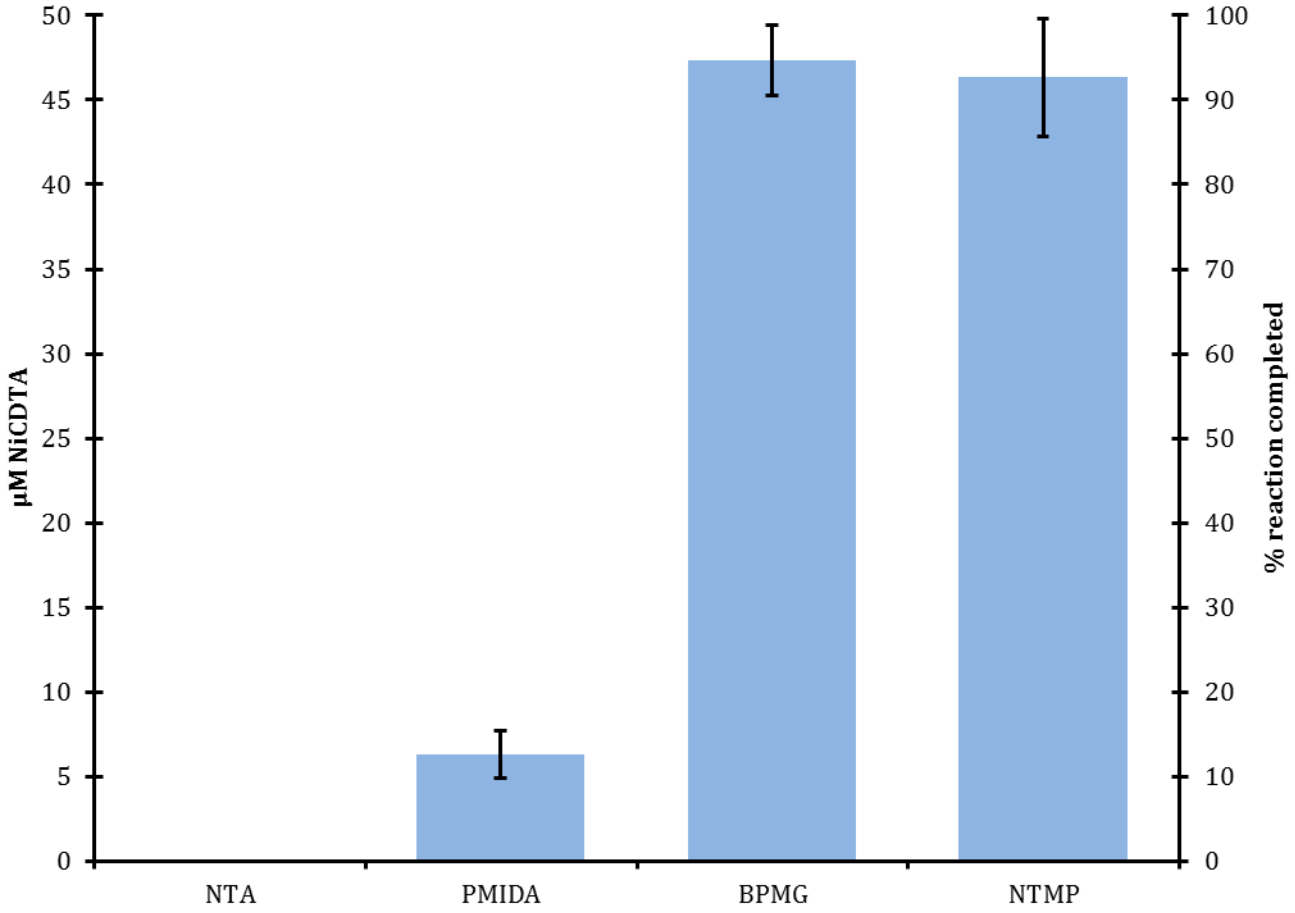

Figure 11. Amount of NiCDTA produced in the reaction NiL + CDTA --> NiCDTA + L after 160 ± 5 seconds (time of 1st CE separation). Reaction conditions: 50 µM Ni_T, 52.5 µM L_T, 200 µM $CDTA_T$,5 mM MOPS (pH 7.0), 10 mM ionic strength.

To explain this observed trend in exchange rate, we must revisit the differences in equilibrium speciation determined from calculations in section 3.4. Most importantly, the predominance of NiHL at pH = 7.0 for BPMG and NTMP means there is a weaker interaction between the protonated phosphonate groups and Ni(II) compared to a deprotonated carboxylate group. One implication of this

change is that (at pH = 7.0) the more phosphonate groups a chelating agents contains, the faster its rate of dissociation (k_d) for a Ni(II) complex may be. For the study of ligand exchange kinetics with CDTA, this leads to the hypothesis that the overall rates of exchange will increase with each conversion of a carboxylate group to a phosphonate. Assuming that a “disjunctive”-type pathway is being followed, the increased dissociation of the phosphonate groups will accelerate the association of CDTA to Ni(II), increasing the overall rate.

3.6 Development of Reverse Injection Method

When analyzing the reaction:

NiPMIDA + CDTA → NiCDTA + PMIDA (22)

it was found that NiPMIDA and NiCDTA have very similar retention times in the capillary because they share the same charge (-2). This similarity resulted in an overlap of their absorbance peaks, meaning that neither could be quantified. To counter this issue, we employed an uncommon technique called reverse (or "short side") injection. This technique has been recently developed and proposed as a simple way to increase analysis speed on traditional (as opposed to microchip or multi-capillary) CE systems.[32] Reverse injection has been utilized in past research performed by Spudeit et al.[33] to determine glycerol concentrations in biodiesel with a very high sample rate. Zinellu et al.[34] also employed reverse injection to investigate levels of serotonin in human blood, and demonstrated improvements in both analysis time and sensitivity for reverse versus normal injection. These two advantages are both applicable to the ligand exchange

reaction involving PMIDA (22). First, the sample plugs of NiCDTA and NiPMIDA are retained in the capillary for a much shorter time before reaching the detector. In a normal injection, the distance traveled by these sample plugs is long enough for them to diffuse enough that they overlap and no longer maintain baseline resolution. In a reverse injection, though, the sample plugs remain sharp until they reach the detector. This allows for baseline resolution and quantification of the peak areas. The second advantage of reverse injection is that separation time can be greatly decreased. Once the specie(s) being analyzed have passed by the detector, the separation can stop and the capillary can be flushed for the next separation. Because the reverse injection technique results in a shorter effective capillary length (length to detector), under the same separation conditions, the species will migrate to the detector much sooner than in a normal injection. This decrease in separation time allows for more separations to be performed in the same amount of time. The results from the first separation experiment indicate that the PMIDA reaction (22) may pose issues for investigation by capillary electrophoresis at pH 7 because of its fast rate. Because the conditions used drove the reaction to 12.6% completion after 3 min, there is a need for more frequent data collection in order to satisfy the requirement for at least 3 data points within the initial rate (20%).

4. Conclusions

In solutions containing metal ions and various chelating agents, the equilibrium speciation can be easily determined from the thermodynamic

properties of the metal complexes which may form. However, as metal ions are exchanged between chelating agents, the speciation will depend on the kinetic control of the ligand exchange reaction. We have determined that the identity of the chelating agent coordination groups affects both the equilibrium and kinetic speciation of systems with multiple chelating agents. More basic groups (e.g. phosphonates versus carboxylates) cause higher concentrations of free Ni(II) and a greater prevalence of protonated (NiHL) complexes. The changes in coordination strength lead to great increases in ligand exchange rates for more basic groups. PMIDA, BPMG, and NTMP all have the same basic tripodal, tetradentate structure as their parent compound NTA, so it can be assumed that they will follow the same disjunctive reaction pathway when reacting with CDTA because of the restrictions imposed by their geometries. More work is required to better characterize the ligand exchange reactions for PMIDA, BPMG, and NTMP, and to determine the dependence of rate on various reaction conditions.

5. Notes for Future Research

5.1 Ligand Exchange Across Varying pH

Varying the buffered pH of NiL solutions with phosphonate containing ligands will alter speciation, as seen in equilibrium calculations of these systems from section 3.4. Increasing the pH from 7.0 will lower the concentration of free Ni(II) and protonated complexes, more closely matching the speciation of the NiNTA system at pH = 7.0, which has a slower ligand exchange rate with CDTA than the phosphonate containing ligands. Data for exchange rates for these

chelating agents with increasing pH can be used to determine whether speciation is the driving factor of the increased rate at pH = 7.0. Additionally, the dependence of the rate on pH (if one exists) can be used to further propose possible pathways the exchange reactions follow.

5.2 Using Different BGEs

Using a buffer other than pyrophosphate in the CE BGE may improve separations. As discussed earlier, the use of MOPS produced better reproducibility between separations, but a faster rate for the same reaction analyzed using a pyrophosphate BGE. Based on this result, we hypothesize that certain BGE buffers (such as MOPS) may affect the rate of reaction. For all reactions performed in this experiment, each sample contained 5 mM MOPS which acted as a pH buffer. When the sample was injected into a capillary containing a 50 mM MOPS BGE, [MOPS] in the presence of the sample increased 10-fold. This corresponding increase in rate indicates that MOPS may be acting as a catalyst in the ligand exchange reaction. To test this hypothesis, an experiment could be performed in which the [MOPS] is varied in the ligand exchange sample to test the rate dependence on [MOPS].

Results gathered using a MOPS BGE could not be directly compared to those gathered using pyrophosphate because a different rate was observed. However, if all of the reactions using different initial chelating agents were all performed using a new BGE, these kinetics results could be compared to each other. Additionally, using a variety of buffers in the BGE could allow for variability

in the pH within the capillary during separation, and could mimic the varying pH of the samples.

5.3 Analysis by Conventional UV-vis

The very fast rates (< 3 minutes at pH = 7) of ligand exchange reactions involving BPMG:

NiBPMG + CDTA → NiCDTA + BPMG (23)

and NTMP:

NiNTMP + CDTA → NiCDTA + NTMP (24)

suggests the need for an alternative analysis method to capillary electrophoresis. Conventional UV-vis systems can collect absorbance spectra on a millisecond timescale, and thus have potential for monitoring these fast reactions through their completion. Chelating agents with similar groups may have similar absorptivity patterns, though. For instance, because CDTA and NTA are both aminocarboxylate chelating agents, they have similar visible spectra, and the Ni(II) complexes they form cannot be differentiated. Therefore, the ligand exchange reaction involving NTA (19) could likely not be monitored by conventional UV-vis. Changing carboxylate groups to phosphonate groups causes a visible spectra shift for the chelating agents and the Ni(II) complexes they form (Figure 12).

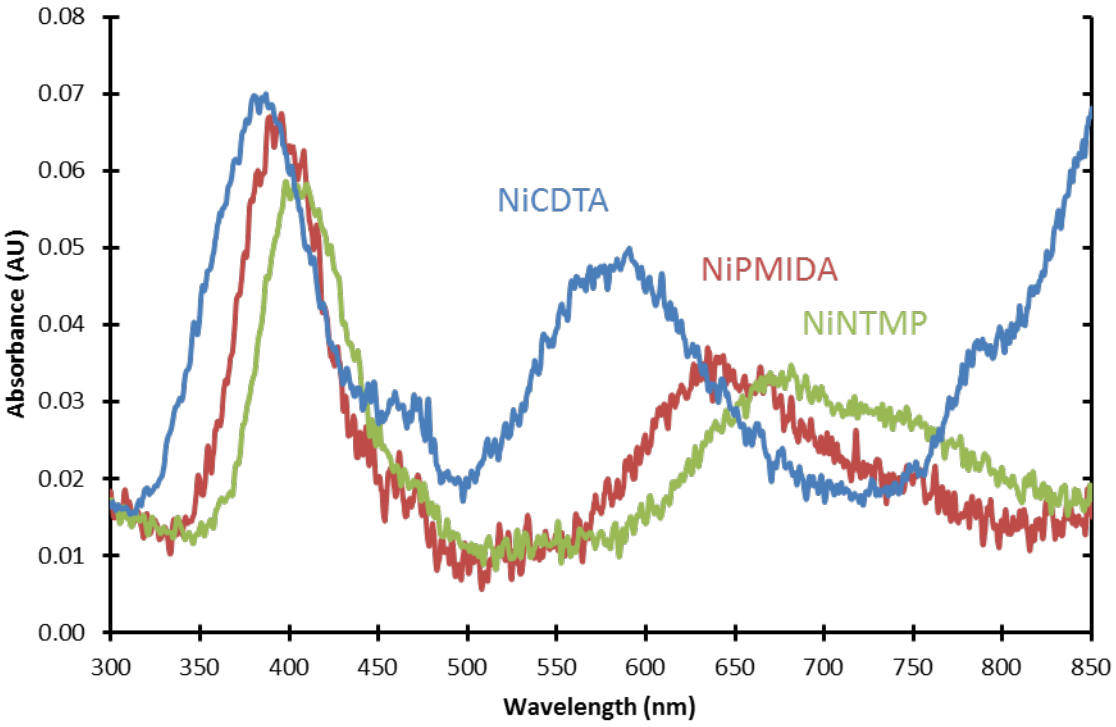

Figure 12. Spectra of different Ni (II) complexes. All complexes have concentration of 5 mM.

There is sufficient separation between λ_{max} for NiCDTA and NiNTMP that, presumably, each could be quantified individually in a sample containing both compounds. Therefore, the separation achieved using capillary electrophoresis is not necessary if these particular components of a sample can be analyzed simultaneously. The capability of continuous monitoring without separation in a conventional UV-vis system is promising for monitoring ligand exchange reactions which occur on time scales too fast for monitoring via capillary electrophoresis.

6. References

(1) Dixon, N. E.; Gazzola, C.; Watters, J. J. Jack Bean Urease, a Metalloenzyme - a Simple Biological Role for Nickel? *J. Am. Chem. Soc.* **1975**, *97*, 4131–4133.

(2) Polacco, J. C.; Mazzafera, P.; Tezotto, T. Opinion: Nickel and Urease in Plants: Still Many Knowledge Gaps. *Plant Sci.* **2013**, *199-200*, 79–90.

(3) Brown, P. H.; Welch, R. M.; Cary, E. E. Nickel: A Micronutrient Essential for Higher Plants. *Plant Physiol.* **1987**, *85*, 801–803.

(4) Temple, P.; Bisessar, S. Uptake and Toxicity of Nickel and Other Metals in Crops Grown on Soil Contaminated by a Nickel Refinery. *J. Plant Nutr.* **1981**, *3*, 473–482.

(5) Kukier, U.; Chaney, R. L. Amelioration of Nickel Phytotoxicity in Muck and Mineral Soils. *J. Environ. Qual.* **2001**, *30*, 1949–1960.

(6) Greenwood, N.; Earnshaw, A. *Chemistry of the Elements*; Elsevier: San Francisco, 2008.

(7) Vallet, V.; Wahlgren, U.; Grenthe, I. Chelate Effect and Thermodynamics of Metal Complex Formation in Solution: A Quantum Chemical Study. *J. Am. Chem. Soc.* **2003**, *125*, 14941–14950.

(8) Drechsel, H.; Metzger, J.; Freund, S.; Jung, G.; Boelaert, J.; Winkelmann, G. Rhizoferrin - a Novel Siderophore from the Fungus Rhizopus Microsporus Var. Rhizopodiformis. *Biol. Met.* **1991**, *4*, 238–243.

(9) Shenker, M.; Hadar, Y.; Chen, Y. Kinetics of Iron Complexing and Metal Exchange in Solutions by Rhizoferrin, a Fungal Siderophore. *Soil Sci. Soc. Am. J.* **1999**, *63*, 1681–1686.

(10) Hoang, T. a.; Ang, H. M.; Rohl, A. L. Effects of Organic Additives on Calcium Sulfate Scaling in Pipes. *Aust. J. Chem.* **2009**, *62*, 927.

(11) Malik, M.; Chaney, R. L.; Brewer, E. P.; Li, Y.-M.; Angle, J. S. Phytoextraction of Soil Cobalt Using Hyperaccumulator Plants. *Int. J. Phytoremediation* **2000**, *2*, 319–329.

(12) Centofanti, T.; Siebecker, M. G.; Chaney, R. L.; Davis, A. P.; Sparks, D. L. Hyperaccumulation of Nickel by Alyssum Corsicum Is Related to Solubility of Ni Mineral Species. *Plant Soil* **2012**, *359*, 71–83.

(13) McNear, D. H.; Chaney, R. L.; Sparks, D. L. The Hyperaccumulator Alyssum Murale Uses Complexation with Nitrogen and Oxygen Donor Ligands for Ni Transport and Storage. *Phytochemistry* **2010**, *71*, 188–200.

(14) Tandy, S.; Bossart, K.; Mueller, R.; Ritschel, J.; Hauser, L.; Schulin, R.; Nowack, B. Extraction of Heavy Metals from Soils Using Biodegradable Chelating Agents. *Environ. Sci. Technol.* **2004**, *38*, 937–944.

(15) Kraemer, S. M.; Crowley, D. E.; Kretzschmar, R. Geochemical Aspects of Phytosiderophore-Promoted Iron Acquisition by Plants. *Adv. Agron.* **2006**, *91*, 1–45.

(16) Takagi, S.; Nomoto, K.; Takemoto, T. Physiological Aspect of Mugineic Acid a Possible Phytosiderophore of Graminaceous Plants. *J. pla* **1984**, *7*, 469–477.

(17) Boland, N. E.; Stone, A. T. CHAPTER 4 - NTA-like versus EDDA-like Chelating Agent-nickel(II) Complexes: The Influence of Connectivity and Rigidity on Ligand Exchange Pathways, The Johns Hopkins University, 2011.

(18) Margerum, D. W.; Cayley, G.; Weatherburn, D.; Pagenkopf, G. Kinetics and Mechanisms of Complex Formation and Ligand Exchange. In *Coordination Chemistry*; Martell, A. E., Ed.; American Chemical Society: Washington, DC, 1978; Vol. 2, pp. 1–220.

(19) Langford, C. H.; Gray, H. B. *Ligand Substitution Processes*; W. A. Benjamin, Inc.: New York, NY, 1966.

(20) Boland, N. E. Chapter 4 - Supporting Information, The Johns Hopkins University, 2011.

(21) Poppe, H.; Xu, X. Indirect Detection in Capillary Electrophoresis. In *High Performance Capillary Electrophoresis: Theory, Techniques, and Applications*; Khaledi, M., Ed.; John Wiley & Sons: New York, 1998; pp. 357–403.

(22) Baker, D. *Capillary Electrophoresis*; John Wiley & Sons: New York, 1995.

(23) Boland, N. E.; Stone, A. T. Chapter 2 - Ni(II) Speciation Determination Using Capillary Electrophoresis. Complexes with Amine- , Carboxylate- , and Phosphonate-Bearing Chelating Agents, The Johns Hopkins University, 2011.

(24) Carbonaro, R. F.; Stone, A. T. Speciation of chromium(III) and cobalt(III) (amino)carboxylate Complexes Using Capillary Electrophoresis. *Anal. Chem.* **2005**, *77*, 155–164.

(25) Wilson, J. M.; Carbonaro, R. F. Capillary Electrophoresis Study of iron(II) and iron(III) Polyaminocarboxylate Complex Speciation. *Environ. Chem.* **2011**, *8*, 295–303.

(26) Bürgisser, C. S.; Stone, A. T. Determination of EDTA, NTA, and Other Amino Carboxylic Acids and Their Co(II) and Co(III) Complexes by Capillary Electrophoresis. *Environ. Sci. Technol.* **1997**, *31*, 2656–2664.

(27) Brooks, S. C. Analysis of Metal-Chelating Agent Complexes by Capillary Electrophoresis. In *Biogeochemistry of chelating agents*; Nowack, B.; VanBriesen, J., Eds.; ACS Publications: Washington, DC, 2005; Vol. 910, pp. 121–138.

(28) McCormick, R.; Zagursky, R. Polyimide Stripping Device for Producing Detection Windows on Fused-Silica Tubing Used in Capillary Electrophoresis. *Anal. Chem.* **1991**, *63*, 750–752.

(29) Papelis, C.; Hayes, K. F.; Leckie, J. O. *HYDRAQL. Technical Report 306*; Stanford, CA, 1988.

(30) Martell, A. E.; Smith, R. M.; Motekaitis, R. NIST Critically Selected Stability Constants of Metal Complexes Database, 2004.

(31) Stone, A. T.; Knight, M.; Nowack, B. Speciation and Chemical Reactions of Phosphonate Chelating Agents in Aqueous Media. In *ACS Symposium Series*; American Chemical Society, 2002; Vol. 806, pp. 59–94.

(32) Glatz, Z. Application of Short-End Injection Procedure in CE. *Electrophoresis* **2013**, *34*, 631–642.

(33) Spudeit, D. A.; Piovezan, M.; Dolzan, M. D.; Vistuba, J. P.; Azevedo, M. S.; Vitali, L.; Leal Oliveira, M. A.; Oliveira Costa, A. C.; Micke, G. A. Simultaneous Determination of Free and Total Glycerol in Biodiesel by Capillary Electrophoresis Using Multiple Short-End Injection. *Electrophoresis* **2013**, *34*, 3333–3340.

(34) Zinellu, A.; Sotgia, S.; Deiana, L.; Carru, C. Reverse Injection Capillary Electrophoresis UV Detection for Serotonin Quantification in Human Whole Blood. *J. Chromatogr. B. Analyt. Technol. Biomed. Life Sci.* **2012**, *895-896*, 182–185.

7. Appendices

7.1 Capillary Electrophoresis Manual (Agilent G1600)

> Starting up the instrument

Turn on the computer and the instrument, and then open the "Instrument 1 Online" software on the PC. In the software UI, open the "Instrument" menu and select "System INIT" to initiate the instrument. Calibrate the UV detector by clicking the "Diode Array" box and selecting "Wavelength Calibration," then manually adjusting the wavelength to the desired value.

> Preparing a capillary and installing the cassette

From the spool of capillary, cut a length of capillary corresponding to the desired total length (length to detector + 7.5 cm) using the measuring tape. To cut, gently score the capillary with the scoring tile and bend to break. According to the measuring tape, mark the section of capillary that will serve as the detector window. This section should be 7.5 cm from the end of the capillary. Align the detector window section of the capillary in the window etching device on a warm hot plate and place a few drops of sulfuric acid on the marked section. Allow the acid to heat up, and then clean the window with ultrapure water, followed by methanol. Slide the window alignment device onto the capillary using the insertion tool and align the stripped piece of capillary in the window. Open the cassette and insert the window alignment device into its slot. Wrap the long end of the capillary around the pegs in the cassette, ensuring the capillary does not come in contact with itself. With the capillary fully in the cassette, close the cassette. Line up the ends of the capillary with the black legs of the cassette,

adjusting its length and position as necessary. Use the magnifying glass and scoring tile to ensure the ends of the capillary are smoothly cut. To install the cassette, click the cassette icon in the software interface and select "Change Cassette." Wait until the buffer vials are moved before opening the CE system. Open the top cover and, if necessary, remove the cassette inside by pulling it towards you and lifting it from the slot. Install the new cassette by inserting it in the slot (making sure the ends of the capillary slide through the holes), then pushing it away from you, locking it in place. Close the top cover and press "Done" on the software interface.

> Capillary Preconditioning

It is necessary to precondition the capillary after it has been stored dry (i.e. at the beginning of each day of operation) or when using a new BGE solution. This serves two purposes: to strip the capillary clean and to equilibrate the capillary wall with the BGE solution. To precondition the capillary: use the method "precond" with vials 2, 4, 5 filled according to the vial chart. This method will flush the capillary for 5 minutes with 0.1M NaOH, 2 minutes with ultrapure water, and for 15 minutes with BGE solution.

> Analyzing a single sample

To run a single sample, or perform a task using a single method (such as preconditioning), make sure “method task” is selected in the top left of the UI. To specify the method which will be performed, choose “load method” under the “Method” menu. If a sample is being run, click the vial icon on the far left of the UI and choose “sample info.” Here, the information for the sample, including its

vial location, the data file any data should be saved as, the folder this data file will be placed in, and any additional info can be entered. It is important to note that all data file and folder names are limited to eight characters. With the proper method loaded and all of the necessary vials filled, the method can be performed by click the large “Start” button.

> Performing a sequence

A sequence can be utilized to run one or multiple samples consecutively. This is necessary for analyzing the kinetics of a reaction. A new sequence can be created under the "Sequence" menu, and formatting a line for each method which will be performed during the sequence. The information needed for each line includes which method will be used, an ID for each sample (if applicable), and the location of each sample (if applicable). If the sequence will be running overnight or past when the lab will be occupied, add the "airdry" method to the end. This will dry the capillary and turn off the lamp. When the same separation inlet and outlet vials are used over and over, enough solution can be transferred from the inlet to the outlet that the volumes are significantly different enough to change the pressure inside each vial. The result of this difference is a change in the electrophoretic mobility, which will affect the migration times of species in your samples. To prevent this phenomenon, the separation vials should only be used for six separations, after which changes in migration time can be observed. Therefore, when preparing a sequence that will use the same sample test method for a high number of separations, a range of methods should be creating, one for each pair of separation vials. Each method can then be used for six

separations before progressing to the next method. Additionally, each set of rinse and waste vials should only be used for about 10-15 consecutive separations to prevent them from emptying, at which point air bubbles could be blown through the capillary. The data files for the sequence can be managed by right clicking the vial tray icon on the far left of the software interface and selecting "sequence parameters." Here, the information for the data files produced by the sequence can be managed. The “subdirectory” will be the folder into which all of the new data files will be placed, and a new folder should be created for each day or experiment. The data files can be automatically created and name by using the “Prefix/Counter” option, which will give the data files increasing subsequent numbers along with your designated prefix. When the sequence has been created, ensure that all the separation, sample, rinse, and waste vials are in place, and then start the sequence.

>> Kinetics sequences

For a kinetics run, make sure the sequence is ready to run (including having all the vials in place except for sample vials). Mix the samples in their vials (and record the time at which you do so), then put them in place and run the sequence. The time you record will serve as the reaction initiation time during data analysis.

> Building methods

A new method can be development by editing an existing method under the “method” menu, or first creating a new method and editing it. This will prompt the following sections in the method development process:

- Comments – This has no impact on the method itself, but can be useful for keeping track of the actions of the method and any edits made to it.
- Home Values – Usually, the lift offset (how high the end of the capillary will be from the bottom of the vials) should be 4 mm and the cassette temperature should be 25°C. The home vials designate which vials will be used as the BGE separation vials in a test method. For other methods that do not involve a separation (such as airdry), these are unimportant.
- Conditioning – Here, the sequence of events that will be performed before and after (pre- and post-conditioning) the injection and then separation of a method can be set. For methods without injections and separation (such as “precond” and “airdry,” this section contains almost all of the instructions for the method. These instructions can be edited in the table by inserting and deleting lines. The different functions that can be performed are: *flush* – rinses the capillary for a set amount of time at the max pressure (930 mbar); *voltage, current,* or *power* – applies a set amount of electricity for a set amount of time; *wait* – the system will idle for a set amount of time; *inlet* or *outlet* – will change the inlet or outlet vial; *pressure* – will apply a set amount of pressure for a set amount of time. Additionally, a function can be found in the “replenish” table which can be used to empty the waste vial. This function should be used during long sequences to ensure that the waste vial does not overfill.

- Injecting – Parameters which will only be relevant for methods involving the injection of a sample. The optimal parameters for reproducible injections have been found to be 35.0 mbar for 15.00 sec.
- Electric – Here, the polarity should be switched to negative for anion detection (positive for cation detection). The voltage should be set to 22-30 kV, based on the BGE conditions, in order to keep the current in a reasonable range (100-150 μA).
- Time Table – Outline what conditions will be monitored during the method. Voltage, current, and temperature should all be selected to ensure they remain constant and at the expected levels. The stop time given here will determine how long the electric field is applied (in other words, the total time of the separation).
- DAD Signals – Details which wavelengths the Diode Array Detector will monitor. For a pyrophosphate BGE with the metal complexes used in this research, the optimal wavelengths are 200, 214, and 254 nm. Also, there is an option to collect an absorbance spectrum across a range of wavelengths which can be viewed for a certain point in time of the separation. This can be useful for determining the best wavelength to use to observe a particular peak.
- Fraction Collection – Useful for separation and collection of different components of the sample into different vials; not used in this research.
- Signal Details – Outline which signals which be saved and for what period of time. The conditions which should be monitored (voltage, current,

temperature) should be selected, as well as all of the wavelengths monitored by the DAD. The start time should be 0 (corresponding to the start of the separation) and the end time should be equal to the separation time.

The remaining sections deal with data analysis, so they can be skipped for now, as data analysis will be addressed later in this manual.

> Analyzing data

To analyze electropherograms, switch the UI mode from “Method and Run Control” to “Data Analysis” in the upper left hand corner. A data file can be opened by choosing the “File” menu, selecting “Load Signal,” and locating the file based on the name given by the method or sequence.

>> Viewing the electropherogram

To zoom in on a specific area of the electropherogram, you can click and drag to draw a box with the “zoom in” option selected, and double click to zoom out. With the “selection” mode, you can click on integrated areas of the electropherogram to highlight their corresponding data in the table.

>> Automatic integration

First, choose the “auto integrate” button under the “Integration” menu. This option automatically sets parameters to find the best fit for integrating the electropherogram. If this does not produce satisfactory integration, the integration parameters can be manually adjusted in the “Integration Events” table, which can be opened by selecting “integration events” under the

“Integration” menu. Here, the following default parameters can be altered in order to produce the most accurate peak integration:

- Slope sensitivity – sets an initial value for peak sensitivity; a lower value will generally be less selective in which peaks are integrated
- Peak width – sets a minimum value for the width of peaks that will be integrated
- Area reject – sets a minimum value for the area of peaks that will be integrated
- Height reject – sets a minimum value for the height of peaks that will be integrated

The following commonly used parameters can also be added to the table and edited:

- Integration on/off – sets a range in the electropherogram in which peaks will or will not be integrated
- Baseline now – sets the baseline for the remainder of the electropherogram to be the value at the given time point
- Baseline hold – draws a horizontal baseline within the time range given, overriding the established baseline; useful for areas where the baseline through a peak may be sloped

>> Manual integration

In some situations, it may be difficult to tweak the integration events in such a way to give reliable areas of peaks. When this is the case, the electropherograms can be easily manually integrated individually (though this

process can turn tedious depending on the number of electropherograms to be analyzed). First, it is helpful to turn off the automatic integration to remove all the now unnecessary information from the UI. Select the “Manual Baseline” icon from the toolbar, and draw a continuation of the baseline underneath the peak which you wish to analyze. This will create a baseline between the endpoints of the line you draw and integrate between the peak and your line. The migration time should be displayed on the electropherogram, and the corresponding peak area should be displayed in the table underneath.

>> Viewing a spectrum

To view a spectrum, open a data file obtained by a method set to collect a spectrum. In the top left of the UI, select “Spectral Task.” Set the reference spectra by selecting “set reference spectrum” under the “Spectra” menu, then choosing a place along the baseline in the electropherogram. Then, the reference-corrected spectrum for a specific peak can be viewed by clicking “select spectrum” under the “Spectra” menu.

> Vial information and diagram

Appendix Table 1. Assignment of vials using methods currently in place at the time of publication in the Agilent G1600 CE system.

Vial	Contents	Method
1	waste	all
2	ultrapure H_2O	Test(1-5) + precond
3	ultrapure H_2O	Test(6-10) + airdry
4	0.1 M NaOH	Test(1-5) + precond
5	0.1 M NaOH	Test(6-10) + airdry
6	BGE (rinse)	Test(1-2) + precond
7	BGE (rinse)	Test(3-4)
8	BGE (rinse)	Test(5-6)
9	BGE (rinse)	Test(7-8)
10	BGE (rinse)	Test(9-10)
11	air	airdry (outlet)
12	air	airdry (inlet)
13/14	BGE (separation inlet/outlet)	Test1
15/16	BGE (separation inlet/outlet)	Test2
17/18	BGE (separation inlet/outlet)	Test3
19/20	BGE (separation inlet/outlet)	Test4
21/22	BGE (separation inlet/outlet)	Test5
23/24	BGE (separation inlet/outlet)	Test6
25/26	BGE (separation inlet/outlet)	Test7
27/28	BGE (separation inlet/outlet)	Test8
29/30	BGE (separation inlet/outlet)	Test9
31/32	BGE (separation inlet/outlet)	Test10
33-47	samples/other	all
48	H_2O (serves as injection outlet)	all methods with injections

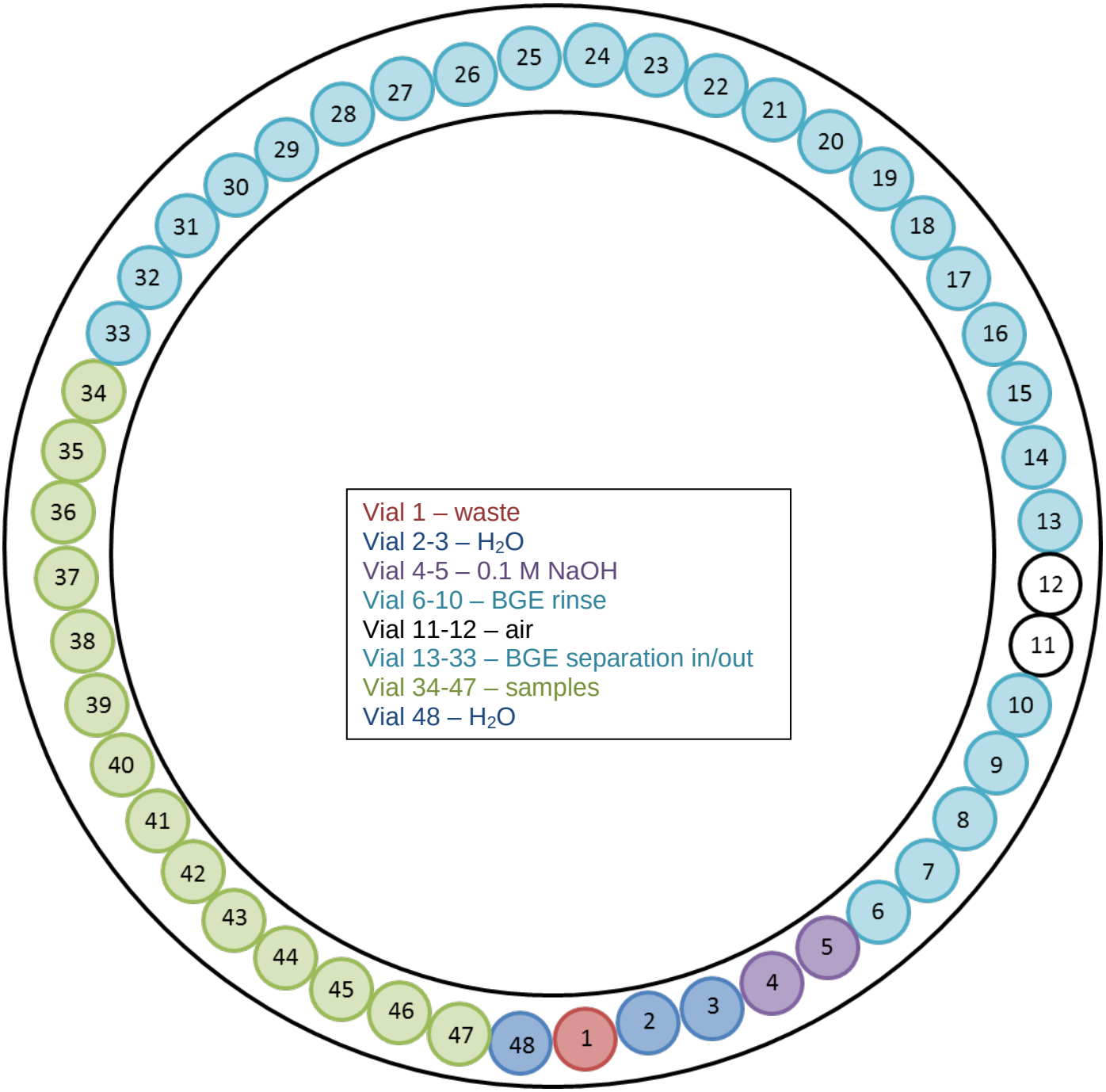

Appendix Figure 1. Assignment of vials using methods currently in place at the time of publication in the Agilent G1600 CE system.

7.2 Experiment Index

Appendix Table 2. Description of various experiments and location of relevant information in notebook.

ID	Description	Page number(s)
TN001	CE calibration & gathering exchange kinetics for NiNTA + CDTA → NiCDTA + NTA	5-28 59-63 (MOPS BGE) 64-68 (Beckman CE)
TN002	Preparation and exchange kinetics of NTA-like amino(carboxylate)phosphonates (PMIDA, BPMG, NTMP)	19-25 30-31 35-37 40-41 63-68 (Beckman CE) 67-68 (reverse injection)
TN003	1st separation data point collection	41-45
TN004	Analysis by conventional UV-vis for phosphonate containing chelating agents	38-40 46-49 58
TN005	Reproducibility and other CE testing	29-39 50-59